Molecular Crystals and Liquid Crystals

Publication details, including instructions for authors and subscription information:
http://www.tandfonline.com/loi/gmcl20

Specific Molecular Motion of Adamantane Induced by Hydrophobic Nanoslits in ACF as Studied Using Solid-State ^{1}H, ^{2}H, and ^{13}C NMR

Hiroaki Omichi [a], Takahiro Ueda [a b], Yu Chen [a], Keisuke Miyakubo [a] & Taro Eguchi [a b]

[a] Department of Chemistry, Graduate School of Science, Osaka University, Toyonaka, Osaka, Japan

[b] The Museum of Osaka University, Toyonaka, Osaka, Japan

Version of record first published: 22 Sep 2010

To cite this article: Hiroaki Omichi, Takahiro Ueda, Yu Chen, Keisuke Miyakubo & Taro Eguchi (2008): Specific Molecular Motion of Adamantane Induced by Hydrophobic Nanoslits in ACF as Studied Using Solid-State ^{1}H, ^{2}H, and ^{13}C NMR, Molecular Crystals and Liquid Crystals, 490:1, 91-105

To link to this article: http://dx.doi.org/10.1080/15421400802305772

Mol. Cryst. Liq. Cryst., Vol. 490, pp. 91–105, 2008

ISSN: 1542-1406 print/1563-5287 online
DOI: 10.1080/15421400802305772

Taylor & Francis
Taylor & Francis Group

Specific Molecular Motion of Adamantane Induced by Hydrophobic Nanoslits in ACF as Studied Using Solid-State ^{1}H, ^{2}H, and ^{13}C NMR

Hiroaki Omichi[1], Takahiro Ueda[1,2], Yu Chen[1], Keisuke Miyakubo[1], and Taro Eguchi[1,2]
[1]Department of Chemistry, Graduate School of Science, Osaka University, Toyonaka, Osaka, Japan
[2]The Museum of Osaka University, Toyonaka, Osaka, Japan

Molecular motion of adamantane confined in activated carbon fiber (ACF) with slit-width of 1.1 nm was investigated using solid state ^{1}H, ^{2}H, and ^{13}C NMR analyses. Temperature dependence of the ^{2}H spin-lattice relaxation time revealed that adamantane undergoes rapid isotropic reorientation in ACF that is much faster than in bulk plastic crystal. Temperature dependence of the line width of the ^{1}H NMR spectrum also suggests that adamantane undergoes translational motion in ACF. The single minimum potential profile between adamantane and the pore wall might engender the high mobility of guest adamantane molecules as a "two-dimensional fluid."

Keywords: activated carbon fiber; adamantane; molecular motion; solid state NMR

INTRODUCTION

Activated carbon fiber (ACF) has homogeneous and hydrophobic slit-type nanopores with slit-width of 1–2 nm [1]. It has large surface area and exhibits strong affinity to many organic molecules. The nanoslit in ACF is regarded as a quasi-two-dimensional nanospace, in which a unique and anisotropic potential field is expected. Such a two-dimensionally restricted space will give rise to a specific state of molecular condensation. In fact, a hexatic phase of carbon tetrachloride (CCl_4) in ACF quasi-two-dimensional nanopore has been observed using the nonlinear dielectric effect [2]. This phase is an intermediate phase, which resembles smectic B liquid crystal. It appears specifically in the two-dimensional molecular arrangement, as predicted by the

Address correspondence to Dr. Takahiro Ueda, The Museum of Osaka University, 1–16 Machikaneyama, Toyonaka, Osaka 560-0043, Japan. E-mail: ueda@museum.osaka-u.ac.jp

KTHNY theory [3]. In this phase, CCl_4 molecules form a two-dimensional layered structure in which each molecule is arranged locally in a pseudo-hexagonal lattice, but not with long-range order among molecules. Consequently, the intermolecular interaction in the anisotropic space makes it possible to provide a specific and particular local structure and dynamics of guest molecules. It is important and desirable to examine a particular and anisotropic molecular assembly of isotropic globular molecule such as CCl_4 in the restricted nanospace from microscopic viewpoints.

Adamantane is a representative globular molecule, of which the diameter (0.76 nm) is larger than that of CCl_4 (0.59 nm) [4]. Adamantane crystallizes the body-centred tetragonal lattice with $a = 6.641$ Å and $c = 8.875$ Å less than 208 K (called *β-phase*). In this phase, the molecular reorientation of adamantane freezes the molecular reorientation, and the molecular orientation is ordered. At temperatures greater than 208 K, the bulk crystal of adamantane changes to a face-centred cubic lattice with $a = 9.54$ Å (called *α-phase*). In this phase, adamantane rotates rapidly, thereby disordering the orientation. The highly disordered structure in molecular orientation is regarded as a kind of smectic D liquid crystal, and is designated as a plastic crystal by Timmermans [5]. This phase has many lattice defects and shows high mobility in the molecular reorientation as well as a large self-diffusion constant, which is two or three orders of magnitude larger than that of normal crystal phase [6]. For example, although the ordinal crystalline self-diffusion constant is *ca.* 10^{-15} m^2 s^{-1} near the melting point, that of adamantane is *ca.* 10^{-13} m^2 s^{-1}. This order of diffusion constants is similar to an intermediate value between a liquid and solid like a liquid crystal.

Restriction of space will affect such physical-chemical properties in bulk adamantane. The quasi-two-dimensional nanospace in ACF will also bring about a hexatic phase of adamantine as CCl_4. Additionally, it is expected to show the specific phase relation of adamantane condensed in ACF nanoslit, which differs from that in bulk because of its anisotropic intermolecular interaction. To date, most previous works have specifically addressed static properties such as the crystal structure and thermal behavior of guest molecules in ACF nanospace [7–9]; however, the effect of confinement on the intermolecular interaction will be evaluated from activation parameters for molecular motion. Solid-state NMR is a useful tool to investigate the dynamic behavior of confined guest molecules in ACF. Furthermore, we have conducted solid-state NMR studies of molecular motion in CO_2 and D_2O confined in ACF [10,11].

In this study, we measured solid-state ^1H, ^2H, and ^{13}C NMR spectra and ^2H spin-lattice relaxation times (T_1) in adamantane and

deuterated adamantane confined in a nanoslit of ACF to examine the molecular motion of adamantane. Temperature dependence of ^{1}H NMR line width and ^{2}H T_1 provided activation parameters of adamantane in ACF. Based on the activation energy, we discussed the intermolecular interaction of adamantane in the ACF nanoslit. Results showed that the confinement in ACF nanoslit enhances the mobility of molecular reorientation as well as the translation of adamantane.

EXPERIMENTAL

Pitch-based activated carbon fiber (ACF20A) was supplied from Osaka Gas Co. Ltd. The porosity of ACF was characterized using N_2 adsorption isotherms; the slit width was 1.1 nm, as described elsewhere [11]. Adamantane was purchased from Wako Pure Chemical Industries Ltd. (Japan). Adamantane-d_{16} (98% atom D) was purchased from C/D/N Isotopes Inc. (Canada). Accommodation of adamantane in ACF was carried out by the following procedure. An appropriate amount of fibre-shaped ACF and adamantane were put into each branch of a Y-shaped glass tube with a needle valve; reduced pressure in the Y-shaped glass tube was achieved using a diaphragm pump. The needle valve was closed; then the Y-shape glass tube was heated to 363 K in a thermostatic bath for 2 days. The resulting sample was mashed to powder; then it was heated again in atmosphere to leave bulk adamantane adsorbed onto the sample surface and co-adsorbed water from humidity. We prepared two samples: one includes adamantane-d_{16}; the other includes normal adamantane as a guest. The adsorption amount of adamantane was estimated using TG-DTA measurements: 0.52 g/ACF 1 g for ACF/normal adamantine; 0.48 g/ACF 1 g for ACF/adamantane-d_{16} samples. The specimens were heated for 4 h at 363 K to leave water from the atmosphere and air in the thermostatic bath. As shown by TG-DTA, the absorbed adamantane were desorbed slightly, then sealed in glass ampoules (5 mm O.D. and 20–30 mm length) with helium gas.

All NMR measurements were conducted using a spectrometer (DSX-200; Bruker Analytik GmbH) operating at the Larmor frequency of 200.13 MHz for ^{1}H, 30.7 MHz for the ^{2}H and 50.3 MHz for the ^{13}C nuclei. For ^{1}H and ^{2}H NMR measurements, the free induction decay (FID) signals were recorded using the solid-echo pulse sequence, which comprises two $\pi/2$-pulses of 4-μs length, a pulse interval of 30 μs, and a repetition time of 4 s (echo top was not observed). The wide-line spectrum was obtained by Fourier transformation of the FID signal. In addition, ^{2}H T_1 measurements were performed using inversion recovery method with a $\pi/2$-pulse and π-pulse of 5 μs and 10 μs.

The ^{13}C NMR spectrum was recorded using a single pulse sequence: $\pi/2$-pulse of 3.5 and 4 μs using 60 and 70 kHz H-decoupling CW pulse and a repetition time of 4s.

Temperature control was achieved by flowing N_2 gas, which was regulated within the experimental error of ± 0.5 K using a temperature controller (VT-3000; Bruker Analytik GmbH).

RESULTS

^{13}C NMR Spectrum of Adamantane in ACF

Figures 1(a) and 1(b) show the ^{13}C wide-line NMR spectra of ACF, including adamantane and of guest-free ACF, observed at room temperature under stationary conditions. In Fig. 1(a), methyene (CH) and methylene (CH_2) carbons in adamantane give rise to isotropic and sharp resonance lines at 25 ppm and 34 ppm, respectively, in spite of observations that were made under no sample spinning with a magic angle. No observation of the anisotropic powder patterns clearly indicates that adamantane molecules undergo isotopic molecular reorientation sufficiently fast to average out the chemical shift anisotropy at room temperature. The ^{13}C chemical shifts of adamantane in ACF are smaller than those in bulk solid (29.5 ppm for CH and 38.5 ppm for CH_2) [12]. These are caused by a ring current effect of

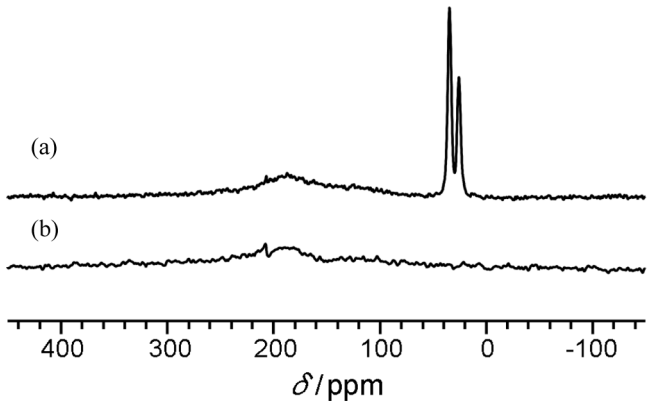

FIGURE 1 ^{13}C-NMR spectra of adamantane in ACF (a) and guest-free ACF (b). A very broad signal around 200 ppm is assigned to ACF carbons. Two narrow signals are assigned to two kinds of adamantane carbon (CH and CH_2). Sharp signal around 210 ppm is spike noise caused by irradiation of the rf pulse.

graphene sheets on the ACF pore surface, strongly suggesting that all adamantane molecules were accommodated in the ACF slit. In contrast, ACF gives rise to a broad resonance line, distributed within 0–300 ppm, as depicted in Fig. 1(b). This broad peak was also observed in the specimen including adamantane, implying that inclusion of adamantane merely changes the structure of the ACF pore wall.

^{2}H Spin-Lattice Relaxation Time of Adamantane-d_{16} Confined in ACF

The inset of Fig. 2 shows the ^{2}H wide-line NMR spectrum of adamantane-d_{16} confined in ACF at 127 K. Even at 127 K, adamantane-d_{16} in ACF gives rise to an isotropic structureless resonance line, strongly suggesting the fast isotropic reorientation of adamantane in ACF. To obtain activation parameters for isotropic molecular reorientation of adamantane-d_{16}, we assessed the temperature dependence of ^{2}H spin lattice relaxation time (T_1) using inversion recovery method. In fact, ^{2}H T_1 is controlled using fluctuation of an EFG tensor, being mainly caused by rotational motion. The large quadrupole-coupling constant (QCC) will engender a short T_1 value, which is unaffected by the

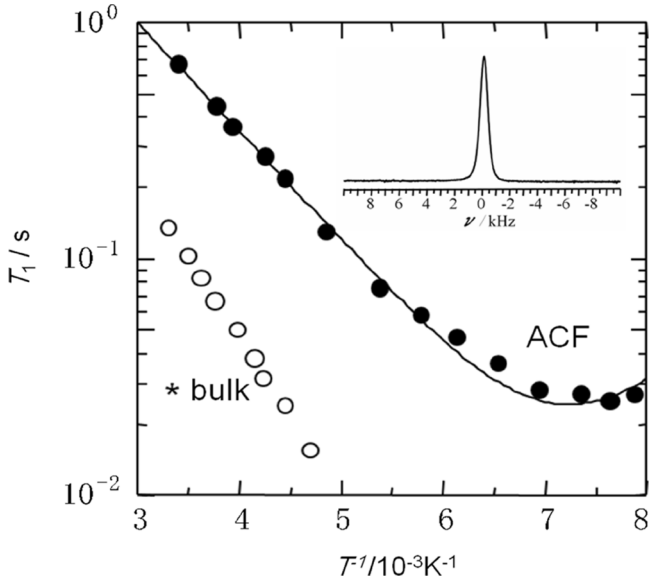

FIGURE 2 Temperature dependence of ^{2}H T_1 of adamantane-d_{16} in ACF20A (●) and bulk (○). The T_1 value in bulk was cited from Ref. 14. The inset shows ^{2}H NMR spectrum of adamantane at 127 K.

paramagnetic component. Therefore, ^{2}H T_1 is favorable for detection of the reorientation of adamantane-d_{16} in paramagnetic media such as ACF. Figure 2 shows the temperature dependence of ^{2}H T_1 for adamantane-d_{16} in ACF. The minimum of T_1 was observed at 135 K, but the lower region was unobservable because of the limitations of our apparatus.

According to Bloembergen, Purcell, and Pound, when the fluctuation of the electric-field-gradient (EFG) tensor results from the molecular reorientation, the inverse of T_1 is represented as the following equation [13],

$$\frac{1}{T_1} = \frac{3}{40}\left(1+\frac{\eta^2}{3}\right)\left(2\pi\cdot\frac{e^2Qq}{h}\right)^2\left[\frac{\tau_c}{1+\omega_0^2\,\tau_c^2}+\frac{4\tau_c}{1+4\omega_0^2\,\tau_c^2}\right], \qquad (1)$$

where e^2Qq/h is a quadrupole coupling constant, η is asymmetric parameter of the EFG tensor and τ_c is the correlation time of molecular reorientation. We assume an Arrhenius-type activation process for molecular reorientation to the temperature dependence of the correlation time,

$$\tau_c = \tau_0 \exp(E_a/RT), \qquad (2)$$

where τ_0 is the pre-exponential factor and E_a is activation energy. Using Eqs. (1) and (2), we reproduced the temperature dependence of ^{2}H T_1, as depicted by the solid line in Fig. 2. In adamantane, the principal axis of the EFG tensor is on the C-D bond; it is good approximation for η to be zero. The reproduced data yielded the following activation parameters for isotropic molecular reorientation of adamantane: 8.8 kJ·mol^{-1} of apparent activation energy (E_a), 1.5 ps of pre-exponential factor of correlation time, and 43 kHz of e^2Qq/h. In fact, Wasylishen *et al*. reported that ^{2}H T_1 in the bulk α-phase implied 174 kHz of e^2Qq/h, 0.1 ps of pre-exponential factor of correlation time, and 13.4 kJ·mol^{-1} of E_a [14]. The T_1 value at the high-temperature side of the minimum is longer than that of bulk solid in the α-phase. This aspect implies that the minimum of V-shaped relaxation curve shifts toward the low-temperature side for adamantane-d_{16} in ACF: reorientation of adamantane in ACF is much more rapid than that in bulk plastic phase. The lower value of E_a in the present study indicates that adamantane in ACF more readily undergoes isotopic molecular reorientation than in bulk α-phase. In addition, the obtained e^2Qq/h value was about a quarter of that reported in bulk, which implies the possibility that other anisotropic motion was excited at a lower temperature than that used to collect our experimental data. The two-dimensionally restricted space in ACF might facilitate the

anisotropic reorientation of globular molecules: the molecular reorientation around an axis perpendicular to the slit-typed pore wall will be easier to observe than that around the axes parallel to the slit-typed pore wall because the friction between adamantane and pore wall will hinder the molecular orientation. Such an anisotropic motion of the globular guest molecules in the anisotropic nanospace was reported in some zeolites: cyclohexane in KL zeolite [15] and MOF-5 [16].

^{1}H NMR of Adamantane in ACF

Figure 3 shows the temperature dependence of the ^{1}H NMR spectrum for the powdered specimen of ACF including adamantane. The resonance line at 150 K consists of at least two components with different line widths. The broader component shows 8.8 kHz of the full width at half maximum (FWHM). The spectrum depends clearly on temperature, and narrows to 0.8 kHz at 270 K. The existence of a temperature-dependent spectrum strongly suggests that the resonance line originates from adamantane. In contrast, the recovery curve of the ^{2}H magnetization can be fitted by a single exponential decay. The ^{2}H quadrupole interaction, which broadens the line width, causes the fast spin diffusion between the subspin systems, probably achieving a single spin temperature in a whole spin system.

In contrast, the ^{1}H NMR spectrum of the dried ACF powder sample without adamantane is presented in Fig. 4. The ^{1}H signal will come

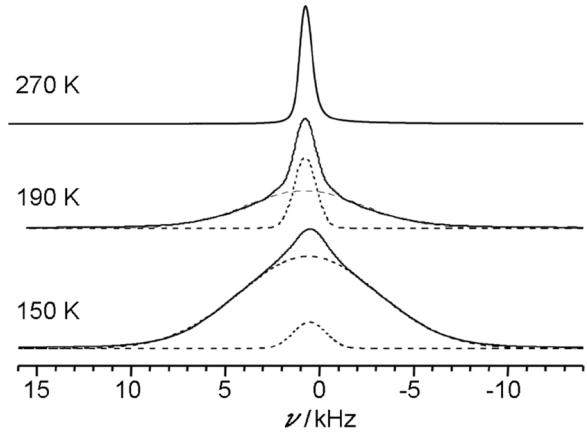

FIGURE 3 Temperature dependence of the ^{1}H NMR spectrum of adamantane in ACF20A. Dotted and dashed lines show two Gaussians using reproduction of the experimental spectrum.

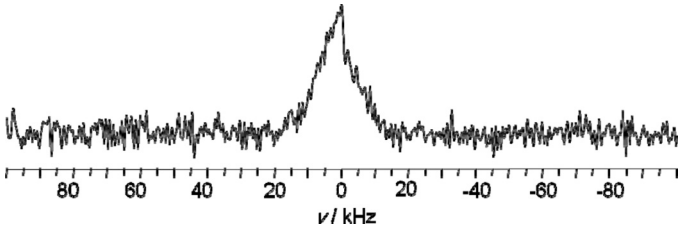

FIGURE 4 ^{1}H NMR spectrum of the dried ACF20A powder specimen observed at room temperature.

from the chemisorbed water as well as the protons bonded to the aliphatic and/or aromatic carbons. The resonance line in the dried ACF sample is much broader than that for the powdered specimen of ACF including adamantane, also suggesting that the narrow and temperature-dependent spectrum in Fig. 3 is attributable to protons in the adamantane molecules. On the other hand, in bulk adamantane, the isotropic molecular reorientation was frozen to less than 150 K; also, the $M_{2\text{rigid}}$ value in a rigid lattice is evaluated as 22 G^2, which corresponds to *ca*. 46 kHz of FWHM for Gaussian resonance line. In this case, the intramolecular contribution of ^{1}H-^{1}H dipolar interaction to $M_{2\text{rigid}}$ is evaluated as 15.8 G^2 (*ca*. 39 kHz of FWHM for Gaussian resonance line) based on the molecular structure of adamantane [18]. The resonance line becomes narrow when the temperature increases. After transition to the plastic phase, the second moments of the ^{1}H NMR resonance line are suddenly reduced; they have a constant value of 0.9 G^2 (*ca*. 9.4 kHz of FWHM for Gaussian resonance line) over the temperature range of 150–500 K. the second moment of 0.9 G^2 results solely from the intermolecular contribution of ^{1}H-^{1}H dipolar interaction because of complete averaging out of the intramolecular ^{1}H-^{1}H dipolar interaction by isotopic reorientation.

Comparing ^{1}H-NMR line width of bulk adamantane with that in ACF, the obtained line width of adamantane in ACF shows that adamantane in ACF is activated more intensely and undergoes molecular reorientation much more rapidly than that of bulk. This feature is consistent with the description of the molecular motion as resulting from the ^{2}H spin-lattice relaxation time. To discuss the molecular motion quantitatively, we examined the temperature dependence of the line width of the ^{1}H NMR spectrum for adamantane in ACF. Although the ^{1}H spin-lattice relaxation time (^{1}H T_1) is commonly used for studying molecular dynamics in solid phase, the paramagnetic species contained in this specimen significantly shortens ^{1}H T_1 and obscures

the contribution of molecular motion to the relaxation mechanism. Because a ^{1}H gyromagnetic ratio is 6.5 times larger than that of ^{2}H, the contribution of T_1 relaxation through ^{1}H-electron dipole interaction is expected to be 42 times larger than that through ^{2}H-electron dipole interaction. However, the ^{1}H line width is generally affected by the net electron spins, which are partially averaged out by the rapid flip-flop motion of electron spins. Moreover, ^{2}H has a quadrupole moment and interacts with the electron field gradient around a nucleus. Since the quadrupole interaction is much larger than ^{1}H-^{1}H magnetic dipole interaction, the spin-lattice and spin-spin relaxation processes are mainly dominated by the quadrupole interaction. Therefore, the paramagnetic effects will be little affected to the ^{2}H T_1 relaxation as well as the line shape for adamantane undergoing rapid isotopic reorientation. The ^{1}H T_1 measurement presents a disadvantage for investigation in graphites and zeolites containing paramagnetic components [19]. Compared to T_1, the line width of ^{1}H NMR is sensitive to the slower molecular motion between 10^{-4} s to 10^{-7} s. In the temperature range of 130–242 K, we reproduced the resonance line at each temperature using superimposition of two Gaussian functions. The ^{1}H NMR signal from ACF itself was not used in the line shape analysis because the resonance line is too broad. At other temperatures, the spectrum was reproduced well using a Gaussian peak. The resultant line widths are shown in Fig. 5 as a function of temperature. As the temperature decreases, the FWHM increases. Appearance of two kinds of resonance lines with different width

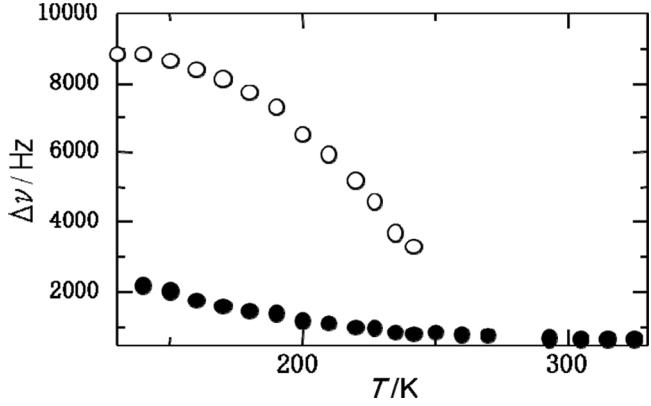

FIGURE 5 Temperature dependence of the full-width at half maximum of the ^{1}H NMR spectrum for adamantane in ACF20A: narrow component (•) and broad component (○).

implies that adamantane forms a domain-like structure in ACF: one is considerably mobile even at less than 150 K; the other has gradually slowing motion to less than 235 K. This probably arises from the inhomogeneous distribution of adsorption sites for adamantane in the ACF slit-type nanopore. Our previous work also pointed out the existence of the inhomogeneous distribution of adsorption sites for CO_2 [11].

Assuming the correlation time of motion controlling line width to be τ_c, the FWHM, $\Delta\nu$, is represented according to a theoretical relationship described by Kubo and Tomita [20], as

$$\Delta\nu^2 = M_{2\text{residual}} + M_{2\text{rigid}} \cdot (2\pi^{-1}) \cdot \tan^{-1}\{2\pi \cdot \tau_c \cdot \Delta\nu \cdot \alpha\}, \qquad (3)$$

where $M_{2\text{residual}}$ is the second moment of the resonance line after the motional narrowing, $M_{2\text{rigid}}$ is the second moment of the resonance line in a rigid lattice, and α is an empirical parameter (usually this is in the order of unity) [21].

For adamantane confined in ACF, two kinds of components are included in the resonance line at less than 235 K. The broader component appears at about 9 kHz at 130 K and decreases gradually to about 3 kHz with increasing temperature. The line width at 130 K is comparable to the line width of bulk adamantane in the plastic phase (*ca.* 9.4 kHz) [17,18]. If line broadening is caused by the isotropic molecular reorientation, the expected line width can be estimated using the correlation time, τ_c, as determined from ^{2}H T_1 measurement. Substituting τ_c and $M_{2\text{rigid}} = 15.8\,\text{G}^2$ into Eq. (3), we obtained $\Delta\nu$ which is approximately equal to $(M_{2\text{residual}})^{1/2}$. Therefore, $\Delta\nu$ is independent of the rotational correlation time at temperatures of 130–235 K: the translational motion of adamantane in ACF, rather than the isotopic rotational motion, will effectively average out the intermolecular ^{1}H-^{1}H interaction.

Furthermore, the narrower component shows slight temperature dependence in comparison to the broader one. The FWHM value changes from 2 kHz at 130 K to 0.8 kHz at 270 K, which implies that adamantane contributing to the narrower resonance line undergoes translational motion in ACF much more readily than that contributing to a broader resonance line.

DISCUSSION

The activation energy of molecular reorientation is given as ^{2}H NMR to be $8.8\,\text{kJ}\cdot\text{mol}^{-1}$, which is less than that in bulk crystal ($12.7\,\text{kJ}\cdot\text{mol}^{-1}$ for α-phase [18], $13.4\,\text{kJ}\cdot\text{mol}^{-1}$ for α-phase-d_{16} [14]

and 27.3 kJ · mol^{-1} for β-phase [18]). This aspect shows that molecular reorientation is easily excited in the ACF nanoslit in comparison to a plastic phase of the bulk solid. The observed E_a value in ACF is closer to that in a solution state than a solid state. Ancian *et al*. reported E_a values of molecular rotation of adamantane in various *n*-alkane solutions. They indicated that the potential barrier for molecular rotation of adamantane is independent of a collision with neighbouring solvent molecules, yielding a constant E_a value of 5.5 kJ · mol^{-1} in various *n*-alkane solutions [22]. They proposed a microscopic picture that adamantane undergoes rotational motion in a cavity composed of neighbouring solvent molecules.

In the ACF slit-type pore, we will discuss the intermolecular interaction between adamantane molecules in terms of the average intermolecular distance between guests, which can be estimated from the pore volume of ACF and the loading amount of adamantane. N_2 adsorption isotherm gives a pore volume of 0.9×10^{-6} m^3/g in ACF20A [11]. Assuming the 2-dimensional hexagonal closed packing of adamantane in the ACF slit (1.1 nm of slit width), the loading amount of guest (0.52 g/ACF 1 g for ACF/normal adamantane and 0.48 g/ACF 1 g for ACF/adamantane-d_{16}) leads to the area that is occupied by a guest molecule; 3.2×10^{-19} m^2 for normal adamantane and 3.9×10^{-19}m^2 for deuterated specimen. Both areas correspond to the area of circle with the radius of 0.34 ± 0.02 nm. That is, the averaged intermolecular distance between adamantane molecules in ACF is estimated to be 0.67 ± 0.03 nm in both specimens. This intermolecular distance is comparable to 0.67 nm for the intermolecular distance between nearest neighbors of adamantine in bulk α-phase (F.C.C). Therefore, it is considered that the friction among guest molecules in ACF is similar to that in the bulk plastic crystal.

Furthermore, we can also discuss the guest-wall interaction using simple model based on the Lennard–Jones 12-6 potential function [23]. This consideration also leads to the expected equilibrium position of adamantane molecules in the slit. Assuming that adamantane is a rigid globular molecule and that the pseudo-two-dimensional nanospace of ACF comprises infinite parallel graphite sheets with slit width R, the potential energy $U(y)$ between a rigid globular molecule and all carbon atoms on the parallel graphite sheets can be modelled using the Lennard–Jones 12-6 potential function as follows [23]:

$$U(y) = (-2\pi\varepsilon n/5)\left(\frac{5(R/2a - y/a)^6 - 2}{(R/2a - y/a)^{10}} + \frac{5(R/2a + y/a)^6 - 2}{(R/2a + y/a)^{10}}\right). \quad (4)$$

Therein, ε is the depth of the potential wall, a represents the position of the zero potential energy, is the sum of the van der Waals radii of the adamantane molecule and the surface carbon atom. In addition, n is the number of surface atoms in an area of a^2. The variable y is the coordinate along the direction perpendicular to the sheet plane; the origin of y ($y = 0$) is at the center of the slit, and $-R/2 < y < R/2$. This function gives the single minimum potential or double minimum potential, depending on the ratio of the slit width (R) to the position of the zero potential energy (a). According to Eq. (4), for $R > 2.4a$, a double-minimum potential begins to develop with a hump at the centre of the slit (Fig. 6) [23]. At smaller R, only a single minimum is located at the centre of potential, *i.e.*, at the center of the slit. For adamantane in the ACF nanoslit, the R/a value is evaluated as 1.2 using $R = 1.1$ nm and $a = (0.76\,\text{nm} + 0.17\,\text{nm})$, which is less than 2.4. Therefore, adamantane will be hindered using a single-minimum potential, and the center of the slit is the stable and equilibrium position for adamantane in ACF. This situation probably reduces the hindrance of molecular reorientation of adamantane by slit walls and facilitates the molecular rotation/reorientation of adamantine, as in the n-alkane solution. Such a potential in the ACF nanoslit will also enable adamantane to jump smoothly in the slit. Based on the consideration, we proposed that adamantane molecules undergo reorientation in the center of slit.

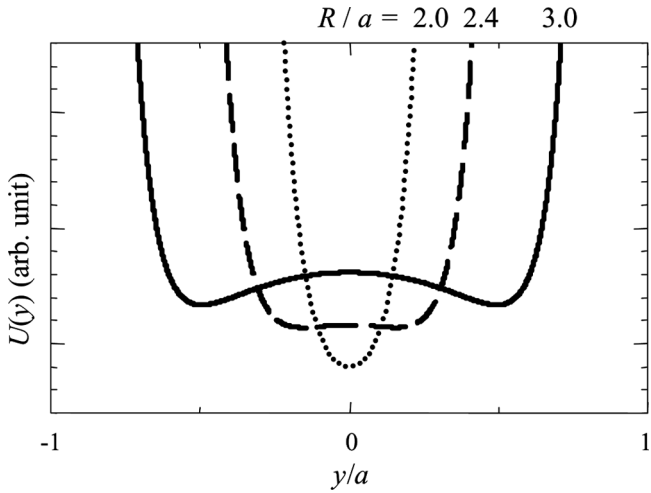

FIGURE 6 Potential energy U(y) of adamantane in ACF nanosite. Those are calculated using Eq. (4). Solid line ($R/a = 3.0$) presents a double minimum potential, whereas dot line ($R/2a$) presents a single minimum potential.

On the other hand, ^{1}H NMR spectra suggest that adamantane undergoes a translational motion, and that at least two kinds of adamantane molecules exist with different rates of motion in ACF. These two components imply the existence of two adsorption sites for adamantane in the ACF nanoslit, as reported in our previous work [11]. Furthermore, the signal intensity of each component depends on temperature: as the temperature decreases, the intensity of the broad peak increases and the intensity of the narrow peak decreases. The population of adamantane occupying each adsorption site depends clearly on the temperature, implying a finite energy gap separating these two sites. When the temperature decreases, adamantane molecules undergoing translational diffusion are trapped in one adsorption site, which is energetically more stable than others. Assuming the Boltzmann distribution to the population of each adsorption site, we can evaluate the energy gap separating these adsorption sites. Figure 7 shows the temperature dependence of the ratio between the populations in each site. The slope of the plot in Fig. 7 gives the energy difference ΔE between two sites as $10\,\mathrm{kJ \cdot mol^{-1}}$. Although this model is very rough because the confined structure is actually more complicated, the value is reasonable for distribution of adsorption energy, as judged from the order of physisorption energy.

An additional remark inferred from results of this work is that adamantane confined in ACF forms a monolayer, as inferred from the pore width (1.1 nm) and the molecular size (0.76 nm). This situation will

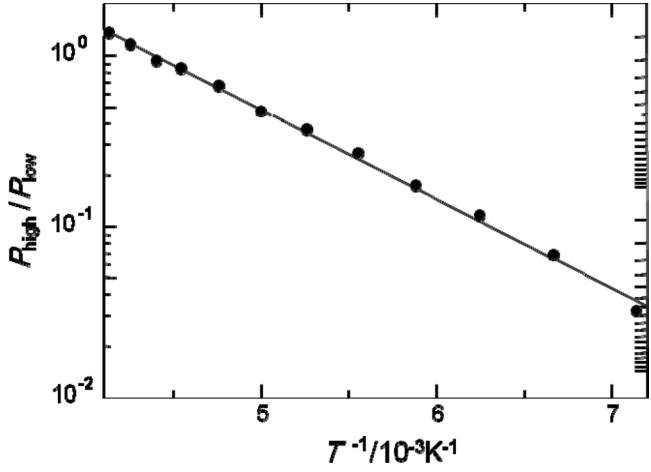

FIGURE 7 Temperature dependence of the population ratio between high and low energy sites.

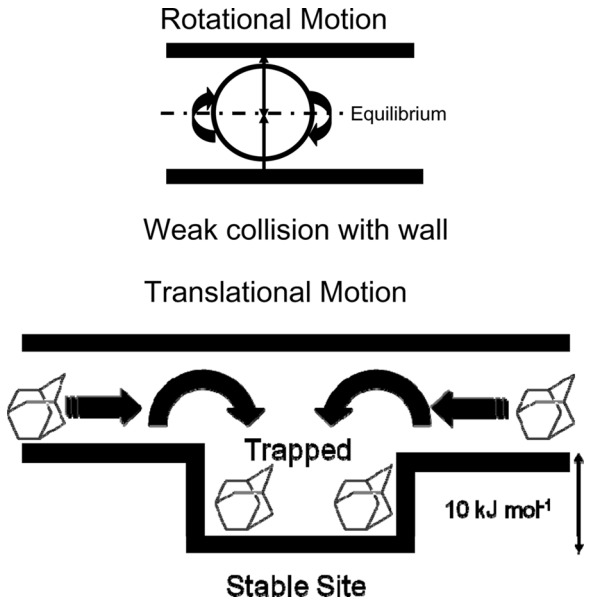

FIGURE 8 Schematic representation of the rotational and translational motions of adamantane in the ACF nanoslit.

bring about the large degree of freedom in the rotation and/or translation of adamantane and the condensed phase of adamantane in ACF might behave as a kind of two-dimensional fluid. Both the single minimum potential peculiar to hydrophobic nanoslits and moderate interaction between adamantane and the pore wall engender such a high mobility of guest adamantane molecules like a plastic crystal phase.

CONCLUSION

This study has particularly examined the molecular dynamics of adamantane being a globular molecule in the nano-slit of ACF. Results obtained using solid state NMR techniques revealed that adamantane in ACF readily undergoes isotopic molecular rotation and translation, suggesting a loose hindrance of adamantane because of the ACF nanoslit. Furthermore, results showed two kinds of adsorption sites in the ACF nanoslit. The energy difference between these sites was evaluated from the temperature dependence of the population of adamantane at each site. Based on these results, we can depict a schematic representation of the molecular motion and the local structure of adamantane in the ACF nanoslit, as shown in Fig. 8. The single

minimum potential between the guest and wall engenders an equilibrium position for the confined adamantane molecules at the centre of the nanoslit. This plays a dominant role in achieving high mobility of adamantane in the ACF nanoslit.

ACKNOWLEDGMENTS

This study was supported by Grants-in-Aid for Scientific Research (16200049 and 16550013) from the Japanese Ministry of Education, Culture, Sports, Science, and Technology.

REFERENCES

[1] Kaneko, K. & Ishii, C. (1992). *Colloids. Surf.*, *67*, 203.
[2] Radhakrishnan, R., Gubbins, K. E., Sliwinska-Bratkowiak, M. (2002). *Phys. Rev. Lett.*, *89*, 076101.
[3] Kosterlitz, J. M. & Thouless, D. J., (1972). *J. Phys.*, *C5*, L124.
[4] Dunnung, W. J. (1961). *J. Phys. Chem. Solid.*, *18*, 21
[5] Timmermans, J. (1961). *J. Phys. Chem. Solid.*, *18*, 1.
[6] Aston, J. G. (1963). *Physics and Chemistry of Organic Solid State*. Wiley: New York
[7] Iiyama, T., Nishikawa, K., Suzuki, T., Otowa, T., Hijiriyama, M., Nojima, Y., & Kaneko, K. (1997). *J. Phys. Chem.*, *101*, 3037.
[8] Suzuki, T., Kaneko, K., & Gubbins, K. E. (1998). *Langmuir*, *13*, 2545.
[9] Sliwinska-Bratkowiak, M., Dudziak, G., Gras, R., Gubbins, K. E., & Radhakrishnan, R. (2001). *Phys. Chem. Chem. Phys.*, *3*, 1179.
[10] Omi, H., Ueda, T., Miyakubo, K., & Eguchi, T. (2005). *Appl. Surf. Sci.*, *252*, 660.
[11] Ueda, T., Omi, H., Yukioka, T., & Eguchi, T. (2006). *Bull. Chem. Soc. Jpn.*, *79*, 237.
[12] Hayashi, S. & Hayamizu, K. (1991). *Bull. Chem. Soc. Jpn.*, *64*, 685.
[13] Abragam, A. (1961). *The Principle of Nuclear Magnetism*, Clarendon Press: Oxford.
[14] Wasylishen, R. E. & Pettitt, B. A. (1980). *Can. J. Chem.*, *58*, 655.
[15] Sato, T., Kunimori, K. & Hayashi, S. (1999). *Phys. Chem. Chem. Phys.*, *1*, 3839.
[16] Ueda, T., Kurokawa, K., Omichi, H., Miyakubo, K., & Eguchi, T. (2007). *Chem Phys Lett.*, *443*, 293.
[17] McCall, D. W. & Douglass, D. C. (1960). *J. Chem. Phy.*, *33*, 777.
[18] Resing, H. A. (1977). *Mol. Cryst. Liq. Cryst.*, *25*, 263
[19] Caro, J., Bulow, M., Schirmer, W., Karger, J., Heink, W., & Zdanov, H. P. (1985). *J. Chem. Soc. Faraday Trans.1*, *81*, 2541.
[20] Kubo, R. & Tomita, K. (1954). *J. Phys. Soc. Jpn.*, *9*, 888.
[21] Andrew, E. R. & Jenks, G. J. (1962). *Proc. Phys. Soc.*, *80*, 633.
[22] Ancian, B., Tiffon, B., & Dubois, J. (1981). *J. Chem. Phys.*, *74*, 857.
[23] Cheung, T. T. P. (1995). *J. Phys. Chem.*, *99*, 7089.